ingegneria sismica
International Journal of Earthquake Engineering
Anno XLIII - Num. 2 - 2026

A Reproducible Laboratory Protocol for Measuring Planck's Constant by LED Threshold Spectroscopy in Undergraduate Physics Education

Le Wang[1], *Jian Huang*[1,2,*], *Zhongwan Dun*[1], *Jianan Zhang*[1] *and Zhihui Wang*[1]

1 Physics; School of Information, Mechanical and Electrical Engineering, Yangtze University College of Arts and Sciences; Jingzhou, 434000 Hubei, China
2 Physics; Jingzhou University; Jingzhou, 434000 Hubei, China

SUMMARY: *Undergraduate Measurements of Planck's Constant using Light-Emitting Diodes (LEDs) are widely employed in current-physics education; however, many classroom variations still exhibit demonstration characteristics or insufficient consistency among different users or students. Developed a reductio ad absurdum lab routine to fix the apparatus shape, changed nominal LED wavelength to be measured by spectrometer peaks; And defined the cutoff voltage by linear extrapolation on the rise section.-voltage curve. Five visible LEDs with nominal wavelengths of 405, 470, 525, 590, and 635 nm were characterized spectrally and measured electrically under controlled conditions. The protocol was executed by six student groups, each completing five independent trials for every LED, yielding 150 threshold records in total. Under the standardized protocol, the pooled threshold-voltage-frequency relation remained strongly linear, with a fitted slope of 4.14 × 10^{-15}V·s, an intercept of -0.064 V, and R^2= 0.999. The corresponding estimate of Planck's constant was 6.63 × 10^{-34}J·s. Group-wise estimates ranged from 6.60 × $10^{-34}$to 6.67 × 10^{-34}J·s, with a mean ± SD of 6.63 ± 0.03 × 10^{-34}J·s. Robustness analysis further showed that the relative error remained below 1.2% when ambient illuminance was kept below 5 lx and the voltage step size was maintained within 10-15 mV, but rose to about 5.8% at 50 lx and 30 mV. Variance ranking identified wavelength assignment (44%) and threshold determination (38%) as the two dominant sources of remaining uncertainty. These results show that the classic LED experiment can be rewritten as a quantitatively stable undergraduate laboratory protocol. Its value lies in making spectral calibration, threshold definition, repeatability, and uncertainty control explicit parts of the teaching task rather than hidden assumptions of a convenient classroom demonstration.*

KEYWORDS: *LED threshold spectroscopy; pLanck's constant; Undergraduate Physics Education; Reproducibility; Laboratory Protocols.*

1 Introduction

Undergraduate modern-physics laboratories are expected to do two things at the same time. Introduce the basic idea of quantum mechanics to students; At this time, present them with an essential relationship between physical constants and an experimental sequence sufficiently detailed to verify it repeatedly, discuss it in depth, etc. Plank's constant also occurs at this point. The revision of the SI has made it clear that h should not be viewed merely as an old symbol in quantum mechanics; It is now part of the base unit definition for measurements. [1, 2] Undergraduate laboratories have multiple educational implications due to the presence of such

*wangle880103@163.com
https://doi.org/10.65102/is2026774
Published: 30 April, 2026

activities; in short, they are necessary. In addition, students need to restore the most reasonable numerical result. In addition, students should understand how to form a good Measurement process through electrical observables, Optical Observers, Fitting Rules and errors.

Among the low-cost routes for experimental teaching Laboratories, led based Experiments have been appealing for many years. It's very obvious in reality. LEDs are low-cost, durable, visually appealing devices that users can easily operate. There are also no ambiguous concepts. Emitting light serves as a clear signal at an electric switch point; by comparing this with the voltage difference across two terminals, we can measure its intensity in photons. The first class-room version of this content used a specific current value that made an LED turn on;[3] Subsequently, there were later revisions that expanded the range of application wavelengths and enhanced electrical reading functionality [4, 5]. Likewise, some related classroom Designs utilised LEDs as Light Sources for photoelectric-effect Demonstrations to demonstrate the function of semiconductor light sources in basic Quantum Physics teaching [6]. Later works have replaced pure visual evaluation with computer-supported collection, more detailed analyses of the current and voltage relationships between LED emissions and semiconductor bands [7-11], etc.

This Development Line enhanced Accessibility; however, this still failed to address the central problem of the experiment's methodology. Many undergraduate realisations have not yet tightened the definition of the threshold voltage operationally. The first bright spark; a current-value approximation for ease of use; A specific point marked by sight on the I-V curve; Or a nominal voltage, such as the turn-on level shown by devices themselves. These options are relatively simple to realise and do not equate precisely. Educational research and classroom materials show that the estimated value of h varies significantly if any of the following factors change: the threshold criterion; whether it takes a wavelength from the colour label or measures through spectrum analysis; And the difference between emitting photons' energy and semiconductor's band gap energy remains unqualified. [12-20] Recently, there have been more refined explanations to add that the practicality of LED-based measurement results is highly sensitive to various minor issues in terms of wavelength allocation, ambient light conditions, voltage step sizes, etc. [21]. Since it needs to be used again repeatedly by different students, these should not be regarded as second-class matters. These factors determine whether it is teaching measurement discipline or merely producing an efficient class number in the experiment.

A second weakness appears at the level of reproducibility. Many LED-based exercises can be successfully presented as demonstrations but have no corresponding reproducibility Laboratory Protocols. The circuit diagram abbreviation is commonly used; When explaining the threshold rule, it will be temporarily connected locally in class; Viewing Geometry has differences at each bench, and Optical Quantity is merely named as a standard-wavelength marked on an LED package. Given these circumstances, it is not certain that all students will have obtained a desired graph; thus, the numerical stability of fitting slopes among them cannot be directly compared. In particular, this gap is more significant within current laboratory pedagogy; that is, measurement uncertainty, source attribution, and interpreting multiple results should not be regarded as important elements in scientific reasoning but merely additional details at the end of calculations. Recently, some scholars' studies of undergraduate laboratory practice have shown that transparent computation analysis helps students understand fitting rules and uncertain factors only when the experiment protocol is relatively stable; 24,25. Reproducibility does not arise due to the application of plotting software alone. Firstly, the way of mounting the LED, methods for measuring wavelengths, ways to increase voltages, definitions of thresholds, all need to be explained to help students collect data later on.

The present study addresses that gap by reformulating the LED experiment as a

reproducible laboratory protocol for undergraduate physics education. The focus is not on obtaining the smallest possible absolute error. It is on constructing a measurement chain that different student groups can execute with comparable decisions and comparable boundary conditions. To do that, the protocol fixes the apparatus layout, replaces nominal wavelength labels with spectrometer-measured peak wavelengths, defines the threshold voltage through linear extrapolation of the rising segment of the I-V response, and constrains the measurement environment through explicit limits on illuminance, temperature, mounting geometry, and voltage-step size. The result is a laboratory exercise that retains the accessibility of the classic LED method while making its operational choices visible and testable.

Three contributions are developed in the paper. First, a standardized apparatus and data-acquisition protocol are specified for five LEDs spanning the visible range, with direct spectral characterization and controlled electrical measurement. Second, the conversion from threshold voltage to Planck-constant estimate is implemented through a fixed analysis path that separates spectral calibration, threshold extraction, regression, and acceptance criteria. Third, the protocol is evaluated through inter-group repeatability, residual structure, uncertainty ranking, and robustness against operating conditions. This keeps the experiment inside the normal resource envelope of undergraduate teaching laboratories, while giving it a more defensible structure for quantitative modern-physics instruction.

2 Methods

2.1 Apparatus Configuration and Spectral Characterization of LEDs

The measurement system was designed around a fixed electrical path and a fixed optical path. Five commercially available LEDs with nominal central wavelengths of 405, 470, 525, 590, and 635 nm were selected to span the visible range with clearly separated colours. Each LED was measured individually inside a matte-black enclosure that limited stray light and fixed the viewing geometry. The LED body was inserted into the same holder for all trials so that lead spacing, mechanical angle, and line-of-sight position did not change from one measurement to the next. A programmable DC supply provided the forward bias, a series resistor constrained the current, and the voltage applied across the LED and the current through the circuit were read simultaneously with digital multimeters. A USB spectrometer was used for spectral characterization, while a lux meter and a temperature probe monitored the ambient state of the enclosure and the benchtop environment.

This arrangement served two purposes. The first was electrical stability. The series resistor and fine voltage control suppressed abrupt current jumps near the onset region and made 0.01 V stepping feasible without overshooting the useful part of the I-V curve. The second was geometric stability. Because the experiment is meant for repeated student use, the optical path could not be left to ad hoc bench placement. The LED mount, spectrometer probe position, and observation window were fixed in advance so that the same device was measured under the same local geometry in every trial. To remove operator-dependent freedom in wiring and positioning, the apparatus and the environmental monitors were fixed before threshold acquisition, as shown in Fig. 1.

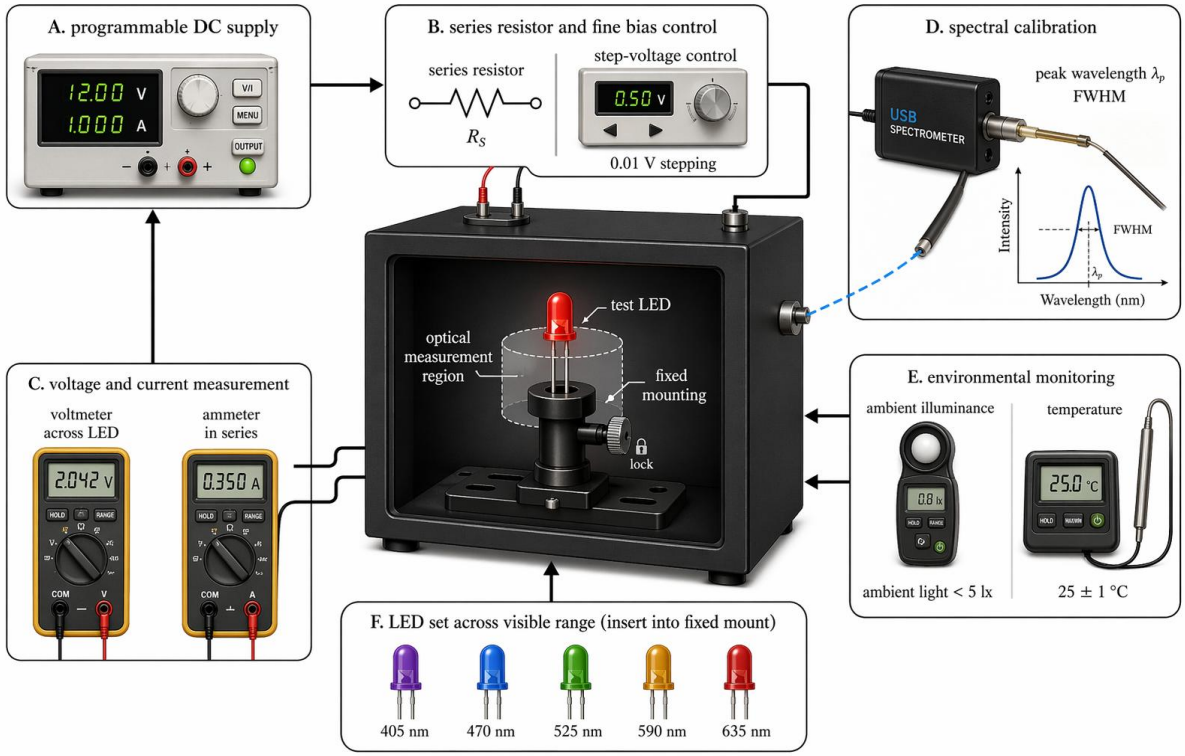

Figure 1: Apparatus Configuration and Spectral Calibration for Reproducible LED Threshold Spectroscopy.

Spectral characterization was carried out before electrical threshold measurements. Each LED was driven at a stable current low enough to avoid visible heating over the acquisition interval but high enough to provide a clean emission peak. After a 30 s stabilization period, ten emission spectra were recorded and averaged. The peak wavelength λ_p was taken from the maximum of the averaged spectrum, and the full width at half maximum was obtained from the half-maximum crossings of the same profile. The measured peak wavelength was then used in the later frequency conversion, rather than the nominal wavelength printed on the component package. This choice matters because nominal colour labels are broad commercial descriptors, while the regression for h depends directly on the frequency assigned to each LED.

Table 1 summarizes the instrumentation and the controlled operating constraints used throughout the study. The list is intentionally modest. No specialized optoelectronic instrumentation beyond a teaching-laboratory spectrometer was required. The reproducibility gain came from fixed operating limits rather than from expensive hardware upgrades.

Table 1: Instrumentation and Controlled Operating Constraints

Instrument / module	Specification used in the protocol	Experimental role	Controlled condition
Programmable DC power supply	0-12 V DC, 1 mV setting resolution	Forward-bias source	Output stabilized before each sweep
Series resistor	100 Ω, ±1% tolerance	Current limiting near onset	Fixed for all LEDs
Step-voltage control	Effective step size 0.01 V	Slow threshold sweep	Same step size in all trials
Voltmeter	0-20 V DC, 1 mV resolution	Measurement of V_f across LED	Parallel connection fixed
Ammeter	0-20 mA DC, 0.001 mA resolution	Measurement of forward current I	Series connection fixed
USB spectrometer	350-800 nm, optical resolution ≈ 1 nm	Measurement of λ_p and FWHM	Same probe position and integration setting
Lux meter	0-200 lx, 0.1 lx resolution	Ambient-light monitoring	Ambient illuminance < 5 lx
Temperature probe	0-50 °C, 0.1 °C resolution	Thermal monitoring	25 ± 1 °C
Dark enclosure with fixed LED holder	Matte interior, constant geometry	Stray-light suppression and repeatable mounting	Same holder and viewing axis for all trials
LED set	Nominal 405 / 470 / 525 / 590 / 635 nm	Visible-frequency sampling	One LED measured at a time

2.2 Threshold-Voltage Extraction and Planck-Constant Estimation

The physical basis of the protocol is the relation between photon energy and optical frequency, together with the empirical relation between LED threshold voltage and emitted light. The analysis started from the standard photon-energy expression shown in Eq. (1).

$$E = h\nu = hc/\lambda \tag{1}$$

For the LED experiment, the threshold relation was written in the working form of Eq. (2), where e is the elementary charge, $V_t h$ is the threshold voltage extracted from the electrical measurement, and φ is an effective offset term that absorbs losses associated with the specific device and the simplified threshold model. Because the frequency assignment was based on measured spectra, the frequency of each LED was computed from Eq. (3), where λ_p is the measured peak wavelength from the spectrometer rather than the nominal manufacturer label. After the LED-specific values of $V_t h$ and ν were obtained, Planck's constant was estimated from the slope m of the linear regression of $V_t h$ against ν through Eq. (4).

$$eV_t h = h\nu - \varphi \tag{2}$$

$$\nu = c/\lambda_p \tag{3}$$

$$h = em, m = dV_t h/d\nu \tag{4}$$

Threshold extraction was more complex than frequency conversion at this time. Increase the forward voltage of each LED successively by 0.01V starting at zero volts. Each time, after settling for 2s at that point, the voltage and current values would be measured separately. Sweeping until the LED entered a state of steady high-brightness emission outside the onset range. No such definition has been established; it is also not based on a certain level of current. Directly identify the effective onset region using the I - V curve. There was no dark-current plateau at low biases, nor any curvature due to increasing-series-Resistanct Effects. Then, a least-squares line was fitted to this ascending section of I > 1; The extrapolated value V_th from it when I →0 will be taken as the initial power. This rule set a level based on the local electrical output of the device, not the person's visual sensitivity.

Two actually invalidations were adopted to reject unstable alignments. The segmented fitting result should be continuous segments of physical monotonicity. Secondly, the linear fitting of each section needed to meet $R^2 > 0.99$ requirements. Those that did not meet the above standard were re-verified in similar environmental Conditions Immediately Afterwards. Photodiode-enclosed starting signals were simultaneously captured for each test item in the condition controller; They are used internally to verify these results. Although this auxiliary trace was not selected to be the primary estimate for V_th; Instead, it offered a separate perspective on when the onset occurred; Additionally, some cases were identified where visual threshold determination might have moved due to background light or observation angle changes.

The last estimated value for h was acquired through two separate means. At the pooled level, the means of thresholds for all LEDs were regressed on their measured optical frequencies to derive one protocol-level slope. At the group level, each student group formed its own V_th-ν, and there was also a group-level - for it. The pooled estimate reflected the average effect achieved by the standardised method; The group-specific ones indicated reproducibility under normal teaching conditions. Since this paper focuses on the problem of protocol stability and not just finding a single optimal curve, both views were kept during all analyses. The threshold-extraction and repeatability-control protocols are depicted in Figure 2.

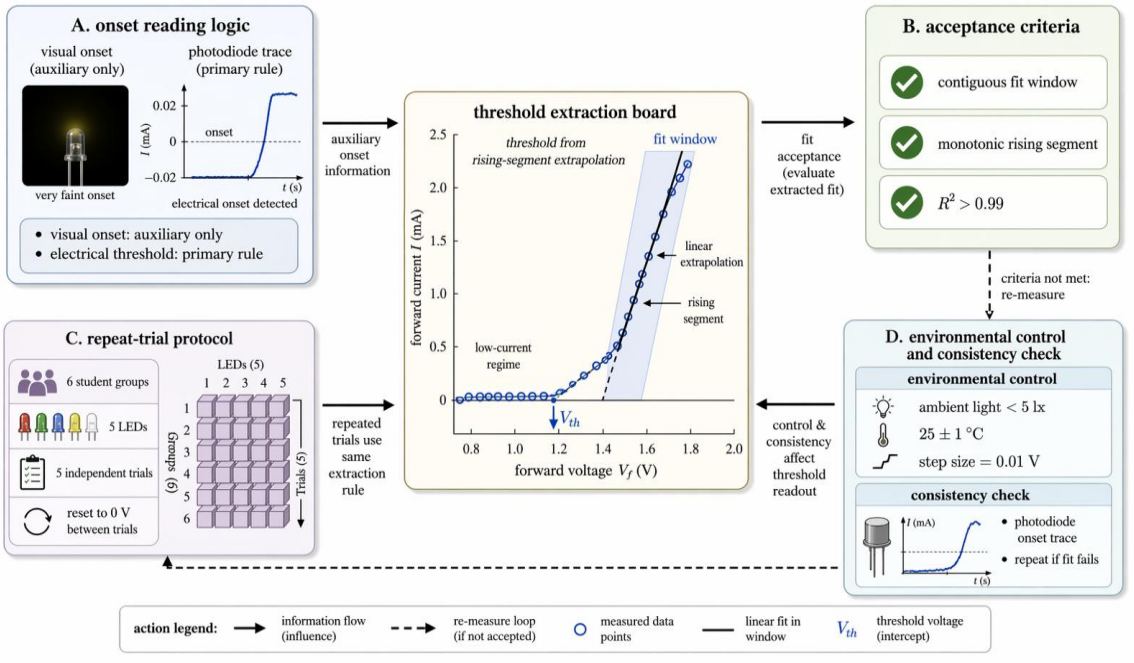

Figure 2: Threshold extraction and reproducibility-control protocol.

2.3 Reproducibility Controls, Trial Design, and Uncertainty Protocol

The experiment organised in this way is not a single performance but several repeatable lab exercises. After conducting a general training session on wiring, data logging, and fit selection for six different students' groups. Each group measured the same five LEDS across five independent experiments. After each trial, the bias was set back to zero; then, re-attach the LED in the same holder as before for use during the teaching laboratory routine. In this Design produced a total of 150 threshold values, each measured at six points (3x5x5). Repetition enabled separation of within-group repeatability and between-groups differences in the protocol.

The environment was controlled to be a method and not explained in terms of background. Before every trial, the LED stayed off for 120s to facilitate adjustment of vision darkness and stabilisation of visual environments close by the box. Ambient Light Intensity Less than 5 Lx. Keep at about 25℃ ±1 ℃ for the laboratory. The same step size of 0.01V was applied to all the standard Runs. All Groups used the same operator instruction; and during the entire experiment, a single mounting position was utilised. Because undergraduates' measurements tend to fluctuate slightly with each repetition due to minor procedural drifts, these controls were selected as straightforward and suitable for routine educational applications to address the primary reasons for differences between bench-to-bench experiments.

V_thV_thv The uncertain policy adopted repetition measurement, residuals analysis, and factor-level disturbance. Repeated measurement provided a standard deviation of for each LED and for each student group. Residual analysis of the pooled - fit identified whether any LED colour systematically departed from the linear model. Next, using factor-level perturbation to obtain the degree of each contributor's impact on system performance: Wavelength Assignment; Threshold Selection; Ambient Light; Temperature Drift; Meter Resolution. Practically, it was to re-perform some measured items after altering one condition in a feasible teaching-lab scope and maintain the other factors unchanged. Normalized and ordered the resulting variances to obtain the respective impacts on each attribute.

As the estimated value of h is extremely dependent on how the threshold is set; therefore, the specific standard for extracting objects and other parameters were agreed upon beforehand, as shown in Figure 2. The following figures present the physical read of the onset area; The linear extrapolation rule; The repeated trial logic; And Environmental limitations were examined later in the robustness assessment.

3 Results and Discussion

3.1 Threshold-Voltage-Frequency Linearity under the Standardized Protocol

The main quantity question of this research is whether after standardising, their lines have the same degree of parallelism with threshold voltages, optical frequencies, and spectral responses to nominal values for LED devices? Based on these two problems are linked. Whether or not there are sufficiently isolated spectral peaks from the selected LED to provide a stable frequency axis. The second, are the extracted thresholds of voltage variation in the I-V curve continuous and roughly straight within the visible light region? The measurement spectra and threshold statistical features of the LED light units are listed in Table 2.

Table 2: Spectral measurement results and threshold statistics for the LED set.

LED color	Nominal wavelength (nm)	Measured peak wavelength λ_p (nm)	FWHM (nm)	Optical frequency ν (×10^{14} Hz)	Mean V_th (V)	SD (V)
Red	635	634.7	18.9	4.72	1.89	0.04
Amber	590	589.3	17.4	5.09	2.04	0.05
Green	525	524.1	28.7	5.72	2.31	0.04
Blue	470	469.6	21.1	6.38	2.58	0.03
Violet	405	404.8	15.2	7.41	3.00	0.04

Alignment between the spectral peak and threshold voltage for the LED array is presented in Figure 3.

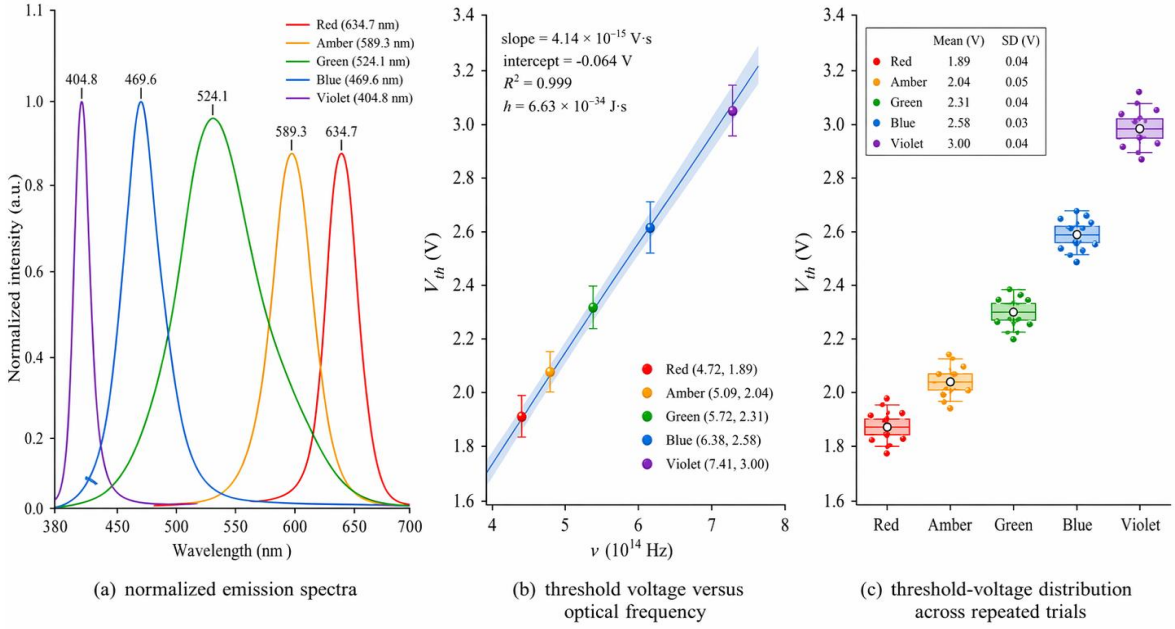

Figure 3: The spectral peaks and threshold-value alignment of the LED set.

Summary of the spectral data and collected thresholds is presented in Table 2, which can also be seen from Figure 3. The measured peaks of the LEDs included a red light LED at 634.7nm, an amber light LED with a wavelength of 589.3nm, a green light LED at 524.1nm, a blue light LED with a peak of 469.6nm, and a violet Light LED with a peak wavelength of 404.8nm. The corresponding optical frequency values are 4.72 × 10^{14}, 5.09 × 10^{14}, 5.72 × 10^{14}, 6.38 × 10^{14}, and 7.41 × 10^{14} Hz, separately. By formulating the standard working protocol, each time was recorded as follows: A, B, C; The average peak voltages of 1.89V, 2.04V, 2.31V, 2.58V and 3.00V appeared respectively; Its corresponding standard deviations had a range between 0.03and0.05Volts). According to what Fig. 3(a) displays, the emission spectra were good separated although visible differences of linewidth exist. The green-light LED had the broadest range, and its full-width at half-maximum (FWHM) was 28.7 nm; The Violet-Light LED had a narrower band width and therefore an FWHM value of only 15.2 nm. The above dissemination has significant implications as it affects the degree of trust in individual's light-emitting diode based on a single measured wavelength.

Convert the measured peaks of wavelength into frequencies; then pool and obtain a corresponding linear response by taking their thresholds. As shown in Figure 3(b). A weighted

linear fitting of V_th versus ν yielded a slope of 4.14 times 10 V cdot s, an intercept of -0.064 V, and R^2 = 0.999. Multiplying the slope by the elementary charge obtained a protocol-level estimation of h = 6.63×10^-34 J•s, with an error of only 0.6% compared to the exact SI value. The sign and size of the intercept matched those that should be present in an effective offset term for the simplified LED threshold model. High Linearity does not constitute evidence that the system is physically complete. However, it is true that under the standardised threshold rule and the spectra-measured frequencies, there existed an adequately consistent dataset suitable for stable undergraduate regression analysis.

Figure 3(c) helps explain why the pooled fit remained stable. The individual distributions of repeated measurement values $V_t h$ are relatively compact and monotonically coloured. Blue-and-purple LEDs were relatively accurate with an absolute error range of±0.03-0.04V; However, amber lights displayed greater fluctuations inaccuracy, exceeding 0.05 V relative errors. It is also in line with the Situation of collecting Data. The onset area of the shorter wavelength LED was more steeply increased and easier to isolate by line extrpolation; The amber onsets were significantly larger with small deviations in procedures. In addition to using measured values, there was another cause of error in classrooms: inferring frequencies simply by examining the nominal positions of LEDs without counting accurately.

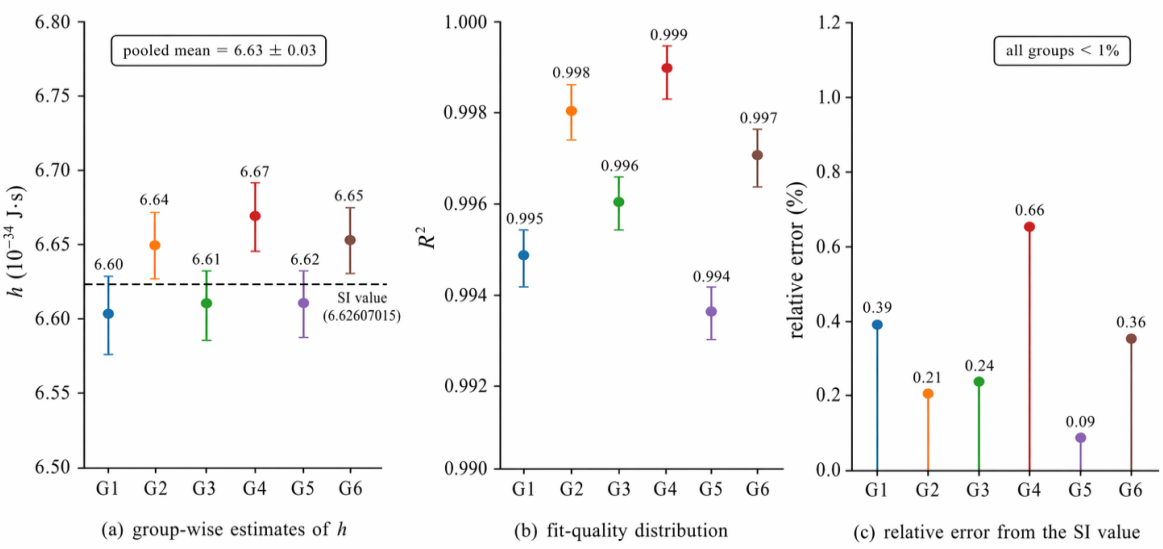

Figure 4: Group inter-stability of threshold fitting and planck constant estimation.

At the group level, to check for the stabilisation of the pooled line, see Figures 4. The six students' groups obtained the values of H as follows: 6.60, 6.64, 6.61, 6.67, 6.62, and 6.65 × 10^{-34} J•s. The groupwise mean is 6.63±0.03×10^{-34}J · s, and the greatest group-level relative error of the group level compared to the SI value was 0.66%. All groups' fitting quality indices were over 0.994 and had excellent fit levels. Therefore, Figure 4 provides an answer to the problem addressed by a single pooled regression analysis alone. The protocol did not generate a single correct signal after combining the data. There emerged a cluster of mutually consistent lines in different groups of students.

3.2 Inter-Group Repeatability and Operating-Window Robustness

The previous subsection established that the standardised protocol had a stable $V_t h$ - ν correspondence relationship. Then, does this stability hold up under repeated tests with the same light source, independent variations in colour temperature, humidity changes in different

environments, etc.? For the purpose of laboratory teaching, this problem is related; a protocol valid in an idealised situation cannot generally be transferred from bench to bench or course to course.

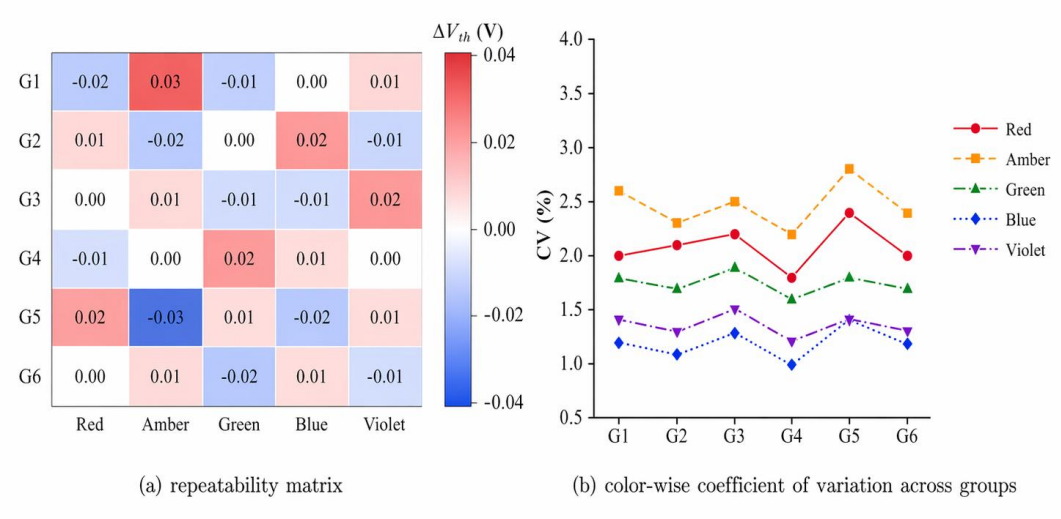

Figure 5: Repetition Matrix of Groups, LEDs and Independent Trials.

The repetitive-trial organisation is shown graphically as follows: As shown in Figure 5a, the normalized threshold-deviations Matrix at all thresholds is presented. Most values were close to the corresponding colours' means plus or minus 0.04V; no groups displayed systematic deviations in all five lights. However, there were still some local concentrations of variation among the amber and red LEDs, particularly in the first two groups after the installation procedure was relatively stable. Figure 5(b) quantifies this pattern through colour-wise coefficients of variation. The pooled within-group cross-validation rate was 1.7%; the colour-specific CV rates were: red (2.1%), amber (2.5%) , green (1.7%), blue (1.2%) and Violet (1.3%). These values are why short wavelength LEDs have affected the fitting curve's trend more significantly. Their ranges of onset were shorter, and the obtained threshold changes slightly with a fixed stepping interval.

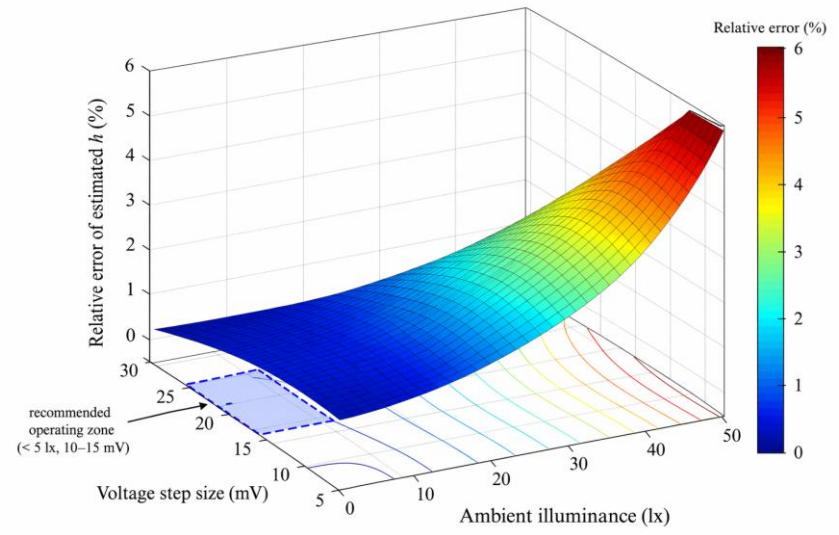

Figure 6: Robust operating window in ambient light and voltage-step disturbance scenario.

Figures of the operating window are as follows. In answer to this practical problem often overlooked in general undergraduates' methods, at which ambient illumination levels combined with voltage-step sizes are sufficient to ensure the system's stability for common applications? In the recommended area, which is ambient light below 5 lux and with a voltage step range of approximately 10 to 15 millivolts, the relative error in estimating h was less than ±1.2 per cent. When the ambient light was higher than 20 lx and the step size exceeded 20 mv, the error surface reached around 3.0%. Near 50 LX and 30 mV in the most negative case, it exceeded five per cent of this value. Therefore, the response surface does not have a flat tolerance area. It has a direct coupling penalty: coarse voltage step and too much ambient light added together.

See Figure 6, which shows that these reasons for choosing the protocol-level constraints. The effect of nearby lights should be reasonable. Any rule for setting a threshold based on the occurrence of either visual or auditory events will be affected by the background contrast in low-light, dark environments. Also have direct impact on the step size. A coarse step moves the onset region to an unobserved poor-quality subinterval; thus, fitting will yield an overestimated intercept and wider confidence bands for the threshold. If both factors change simultaneously, it will become more difficult; poor onset contrast and sparse voltage sampling operate in the same local area of the I-V curve. 3D-robustness Surface is not only a graph but also other functions. There is a teaching-lab Operating Window that can be specified beforehand and verified during its use.

Combining Figs. 5 and 6, it can be seen that the repeatability of this experiment is influenced less by extraordinary instruments than by meticulous control over a relatively few ordinary variables. Inter-group spread remained relatively small when the mounting, illuminance and stepping regulations were set. When those controllers are reduced under the perturbation analysis, the fitted value of h moves rapidly. The difference that this present protocol aims to bring out is explicitly shown here.

3.3 Error Sources, Pedagogical Meaning, and Transferability of the Protocol

Finally, we need to find out where the final error lies and what it specifically signifies in terms of university students' practical application? Without realising that it has shortcomings, this process will also not be reproducible. Therefore, the final section of this analysis focused on residual structures, ranked the uncertainties based on their contributions, and compared different sets of threshold values.

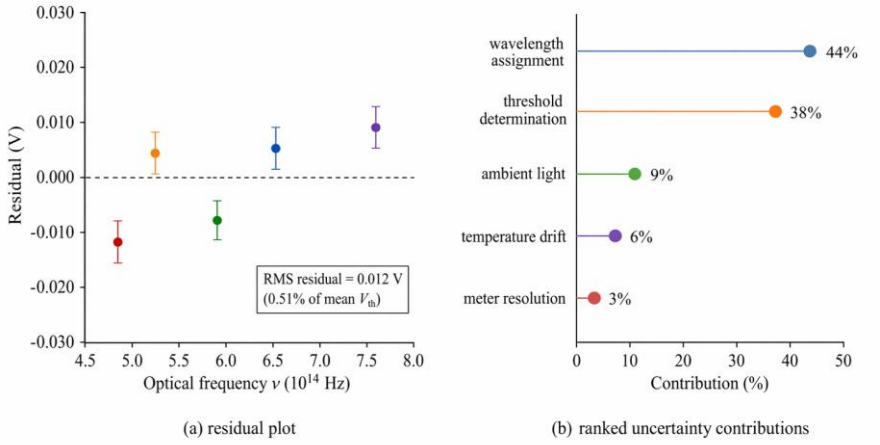

Figure 7: Residual structure and ranked uncertainty contributions of the standardised protocol.

Figure 7a displays the residual results of the pooled linear fit. Residuals were relatively small in value and had no directionally significant changes; The RMS residuals were only 0.012V, accounting for only 0.51% of the mean threshold voltages. As shown in this way, there are relatively minor differences among various devices; these variations do not stand out as large deviations from average performance but rather spread across multiple components. Figure 7b shows the ranking of cumulative explanatory power for observed variability. Wavelength assignment was the primary cause of failure, accounting for 44%; Second place: Threshold determination; Ambient light:9%; Temperature drift: 6%; And meter resolution accounted for less than 3%. The Ordering is organised logically. Finally, the two coordinate axes of the regression are obtained by grouping each point's frequency according to the onset criteria separately. Stable after this point, they have an additive relationship over time.

Table 3 records the groups of repeatability index along with the full relative error and fitting degree. The combined calculated value of h was $6.63 \pm 0.03\times10^{-34}$ J·s, its combined average R^2 is 0.997; And the proposed operating region still surrounds the light source with less than 5lx at each voltage increment of 10~15mV. The above Table has utility here as it integrates several aspects of the work effect of protocols that are often reported separately: proximity to the commonly known numerical value, correlation degree and repeatability across various groups.

Table 3: Group-wise Reproducibility, relative error and uncertainty summary.

Group	Estimated h ($\times10^{-34}$ J·s)	Relative error (%)	Mean R^2	Within-group CV (%)
G1	6.60	0.39	0.995	1.9
G2	6.64	0.21	0.998	1.5
G3	6.61	0.24	0.996	1.8
G4	6.67	0.66	0.999	1.3
G5	6.62	0.09	0.994	2.1
G6	6.65	0.36	0.997	1.4
Pooled	6.63 ± 0.03	0.06	0.997	1.7

Pooled RMS residual = 0.012 V; Recommended operating window: Ambient Light <5 lx, Voltage Step Size (step) between 10 to 15 mV.

Figure 8 shows that there are differences in the threshold rules, and therefore, it is possible to see one's main idea through them. The student group mean when the threshold was set according to a straight line extending from the peak was $6.63\pm0.03\times10^{-34}$ J·s. Photodiode onset rule gave a value of $6.59 \pm 0.05\times10^{-34}$J·s, still within the range but relatively more scattered. A fixed-current constraint was imposed as a general starting-point current, which underestimated by about 6.5% (95% confidence interval: $6.50 \pm 0.08\times10^{-34}$ J·s). Only a pure visual-onset rule overestimated the quantity and spread more widely to some extent, giving $6.74\pm0.14\times10^{-34}$ J•s. Therefore, Figure 8 illustrates the reason for the Protocol level definition of threshold. Different threshold rules do not merely add random scatter. They also move the centre point for estimating differently.

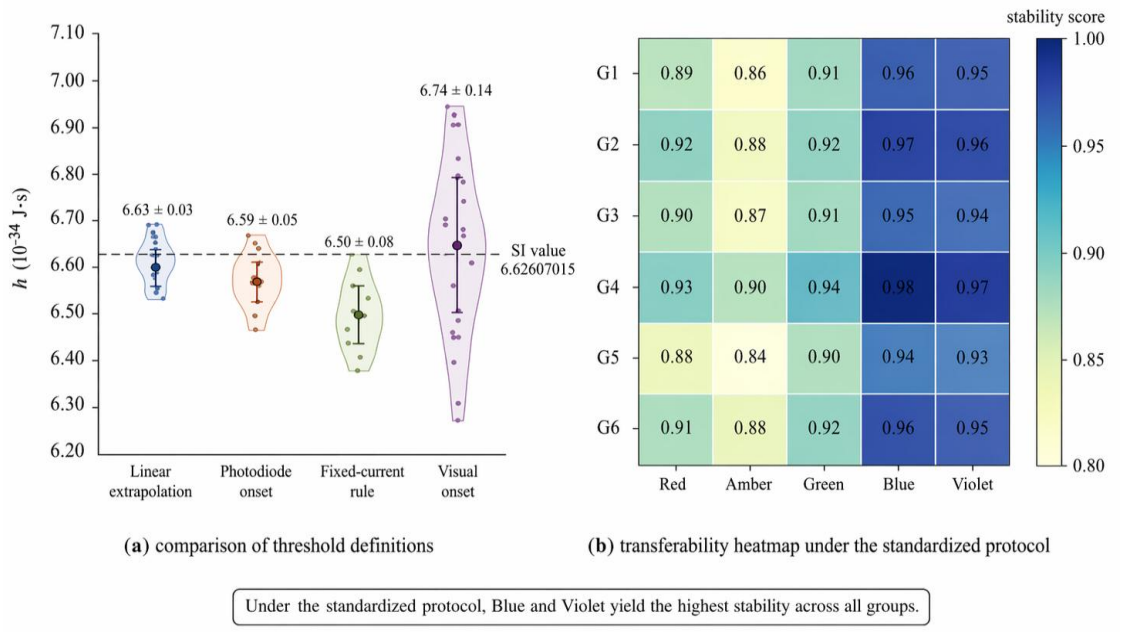

Figure 8: Comparison of Thresholds' Definitions and Transferabilities for Protocols.

Pedagogical outcomes are immediate effects. LED-based measurement of h is usually popular among undergraduates for its easy visualisation, the ability to wire the circuit independently, and fitting a single straight-line segment. These advantages still exist in the current protocol, but organised by discipline of measurement. Although students have access to an inexpensive quantum device, they need to differentiate between nominal and measured wavelengths; between observed onset time and actual operating point; and among one correct plot and a repeated verification success. Therefore, it is more in line with the current view that Laboratory Learning aims to cultivate students' ability for uncertainty reasoning and protocol transparency within their concept-building stage.

Transferrability is also a benefit in this case. The device is still in line with normal teaching-lab equipment; Data analysis may use common regression software or transparent Python codes. The first-order need of procedural adaptation. It is also not the case that in any given laboratory, all the LED devices have identical fitted values to one decimal place at this time. Device-specific emission properties, broad spectral asymmetry and thermal behaviour beyond the test range will also be affected. The results of what we have shown are that a relatively minor set of explicit control measures can be applied to the classic LED experiment so that it transforms into a repeatable undergraduate exercise with an established uncertainty framework.

4 Conclusion

Reorganising the traditional LED experimental set-up to measure Planck's constant as a standard lab activity in an undergraduate Physics course. Mainly, we did not need to provide a sufficiently large range of values for estimating h, merely maintaining consistency across all measurements. To achieve this objective, the geometry of the equipment needs to remain unchanged; after taking a spectrum with it, we should have clear rules for determining thresholds; multiple rounds of trial operation should be conducted by different students' groups; finally, ranking processing of uncertainties should be carried out. According to this experimental method, there was a direct relationship between the threshold voltage and optical frequency for all five types of LEDs; after calculating using Planck's law, we obtained H =

6.63×10^{-34} Js, which had an absolute error of ±0.06% from the precise SI unit.

(1) The work organised an undergraduate experiment along the lines of having a traceable set of objects and Measurements rather than loose classroom demonstrations. FIVE Leds were spectrally characterised, with threshold voltages obtained from standardised I-V curves; The entire data set was conducted in five students' group and each Led had a total of five individual experiments. To provide a data structure adequate for discussion of repeatability and more than one final regression line.

(2) Based on this finding, it can be determined that the best option is among these two options of assignment for wavelength and definition for thresholds; respectively. The standardization rule used spectrometer-measured peak wave lengths and straight line outward extension of the ascending part of the I-V curve. The above selection has provided precise threshold distribution results with an excellent match rate and a mean value at the group level of $6.63\pm0.03\times10^{-34}$J•S. Robustness analysis have also revealed that there is a practicable working area under 5 lumens of light intensity and within ±10~±15mV range for voltages at the teaching laboratory guidance manuals could be filled directly.

(3) There is a relatively evident limitation that can guide further improvement. Although many older standards retain some characteristics of traditional commercial LCD displays; It is difficult to eliminate the problem of sharp wavelength deviation due to erroneous spectral information and its narrow application range at room temperature. Wide verification in various Institutions involving changes to the light source or spectrophotometer model would further confirm its validity. Although there are limitations, these results show that the LED experiment still retains its quantitative responsibility for undergraduates' laboratories under certain operation selections being specified explicitly and integrated into the content analysis of this experiment.

Funding

Hubei Provincial Department of Education Teaching and Research Project Grant ID: 2025567

References

[1] Supreme People's Court. (2022). Opinion on regulating and strengthening artificial intelligence judicial application.

[2] CEPEJ. (2018). European ethical charter on the use of artificial intelligence in judicial systems and their environment. Council of Europe.

[3] UNESCO. (2025). Guidelines for the use of AI systems in courts and tribunals. Paris: UNESCO.

[4] National Institute of Standards and Technology. (2023). Artificial intelligence risk management framework (AI RMF 1.0) (NIST AI 100-1).

[5] Cui, J., Shen, X., & Wen, S. (2023). A survey on legal judgment prediction: Datasets, metrics, models and challenges. IEEE Access, 11, 102050-102071.

[6] Feng, Y., Li, C., & Ng, V. (2022). Legal judgment prediction: A survey of the state of the art. In Proceedings of the Thirty-First International Joint Conference on Artificial Intelligence (pp. 5461-5469).

[7] Xiao, C., Zhong, H., Guo, Z., et al. (2018). CAIL2018: A large-scale legal dataset for judgment prediction. arXiv, arXiv:1807.02478.

[8] Liu, Y., Wu, Y., Zhang, Y., et al. (2023). ML-LJP: Multi-law aware legal judgment prediction. In Proceedings of the 46th International ACM SIGIR Conference on Research and Development in Information Retrieval (pp. 1023-1034).

[9] Wu, Y., Zhou, S., Liu, Y., et al. (2023). Precedent-enhanced legal judgment prediction with LLM and domain-model collaboration. In Proceedings of the 2023 Conference on Empirical Methods in Natural Language Processing (pp. 12060-12075).

[10] Fei, Z., Shen, X., Zhu, D., et al. (2024). LawBench: Benchmarking legal knowledge of large language models. In Proceedings of the 2024 Conference on Empirical Methods in Natural Language Processing (pp. 7933-7962).

[11] Li, H., Chen, Y., Ai, Q., et al. (2024). LexEval: A comprehensive Chinese legal benchmark for evaluating large language models. Advances in Neural Information Processing Systems, 37, 25061-25094.

[12] Zhang, Y., Huang, W., Feng, Y., et al. (2024). LJPCheck: Functional tests for legal judgment prediction. In Findings of the Association for Computational Linguistics: ACL 2024 (pp. 5878-5894).

[13] Han, Z., Yang, Y., Feng, Y., et al. (2025). LawShift: Benchmarking legal judgment prediction under statute shifts. In NeurIPS 2025 Datasets and Benchmarks Track.

[14] Zhang, K., Yang, H., Tang, X., et al. (2025). Beyond guilt: Legal judgment prediction with trichotomous reasoning. In Findings of the Association for Computational Linguistics: EMNLP 2025 (pp. 1815-1826).

[15] Ryberg, J. (2025). Criminal sentencing and artificial intelligence: What is the input problem? Criminal Law and Philosophy, 19(2), 203-220.

[16] Ryberg, J. (2025). Artificial intelligence and criminal justice: How to use algorithmic sentencing support in real life (and ethically non-ideal) penal systems? AI and Ethics, 5, 3255-3263.

[17] Kiejnich-Kruk, K., Twardawa, M., & Formanowicz, P. (2025). Overcoming sentencing inconsistency: A proposal for algorithmic guidelines and juridical misalignment index. Artificial Intelligence and Law.

[18] Rodger, H., Lensen, A., & Betkier, M. (2023). Explainable artificial intelligence for assault sentence prediction in New Zealand. Journal of the Royal Society of New Zealand, 53(1), 133-147.

[19] Zhao, Q. (2025). Legal judgment prediction via legal knowledge extraction and fusion. Journal of King Saud University - Computer and Information Sciences, 37, 31.

[20] Shen, Y., Wei, H., & Tian, X. (2025). TA-LJP: Term-aware legal judgment prediction. Information, 17(1), 17.

[21] Shi, W., Zhu, H., Ji, J., et al. (2025). LegalReasoner: Step-wised verification-correction for legal judgment reasoning. In Proceedings of the 63rd Annual Meeting of the Association for Computational Linguistics (pp. 7297-7313).

[22] Mei, Z., Zhan, C., Ye, W., et al. (2026). Legal judgment prediction based on charge-anchored graph constraints. Expert Systems with Applications, 302, 130480.

[23] Berk, R. A., Kuchibhotla, A. K., & Tchetgen Tchetgen, E. (2024). Improving fairness in criminal justice algorithmic risk assessments using optimal transport and conformal prediction sets. Sociological Methods & Research, 53(4), 1629-1675.

[24] Santosh, T. Y. S. S., & Chowdhury, I. (2025). Fairness beyond performance: Revealing reliability disparities across groups in legal NLP. In Proceedings of the 63rd Annual Meeting of the Association for Computational Linguistics (pp. 24376-24390).